Brief Report

Oral epithelial cells expressing low or undetectable levels of human angiotensin-converting enzyme 2 are susceptible to SARS-CoV-2 virus infection in vitro

Laith Ebraham[1#], Chuan Xu[1#], Annie Wang[1], Divino Rajah[3], Lewins Walter[3], Salvatore A. E. Marras[1,2], Sanjay Tyagi[1], Daniel H. Fine[4*], Carlo Amorin Daep[3*] and Theresa L. Chang[1,2*]

[1]Public Health Research Institute, [2] Department of Microbiology, Biochemistry and Molecular Genetics, New Jersey Medical School, Rutgers, the State University of New Jersey, Newark, NJ, 07103, USA; [3] Global Technology Center, Colgate-Palmolive Company, Piscataway, NJ, 08855, USA; [4]Department of Oral Biology, School of Dental Medicine, Rutgers, the State University of New Jersey, Newark, NJ, 07103, USA.
# These authors contributed equally.
* Correspondence: Theresa L. Chang, PhD. Public Health Research Institute, Rutgers, New Jersey Medical School, 225 Warren Street, Newark, NJ 07103, USA. Email: Theresa.chang@rutgers.edu; phone: 973-854-3265 fax: 973-854-3101;
Carlo Amorin Daep, Ph.D. Senior Principal Scientist; Colgate-Palmolive Company, Oral Care Research and Innovation, Global Technology Center; 909 River Road D133L, Piscataway, NJ 08855, USA,
Email: carlo_daep@colpal.com; W: 732-878-7237; M: 502-295-1449;
Daniel H Fine, DMD; Rutgers School of Dental Medicine, Rutgers University, MSB Rm C-636, 185 South Orange Avenue, Newark, NJ 07103, USA, Email: Finedh@sdm.rutgers.edu, phone: 973-972-3728, fax: 973-972-0045

Abstract: The oral cavity is thought to be one of the portals for SARS-CoV-2 entry. Because there is limited evidence of active oral infection by SARS-CoV-2 viruses, we assessed the capacity of SARS-CoV-2 to infect and replicate in oral epithelial cells. Oral gingival epithelial cells (hTERT TIGKs), salivary gland epithelial cells (A-253), and oral buccal epithelial cells (TR146), which occupy different regions of the oral cavity, were challenged with replication competent SARS-CoV-2 viruses and with pseudo-typed viruses expressing SARS-CoV-2 spike proteins. All oral epithelial cells expressing undetectable or low levels of human angiotensin-converting enzyme 2 (hACE2) but high levels of the alternative receptor CD147 were susceptible to SARS-CoV-2 infection. Viral dynamics in hTERT TIGKs were different from those in A-253 and TR146 cells. For example, levels of viral transcripts were sustained in hTERT TIGKs but were significantly decreased in A-253 and TR146 cells at day 3 after infection. Analysis of oral epithelial cells infected by replication competent SARS-CoV-2 viruses expressing GFP showed that the signals of GFP and SARS-CoV-2 mRNAs were not evenly distributed. Taken together, our results demonstrated oral epithelial cells were susceptible to SARS-CoV-2 viruses despite of low or undetectable levels of hACE2, suggesting that alternative receptors contribute to SARS-CoV-2 infection and may be considered for development of future vaccines and therapeutics.

Key word: SARS-CoV-2; oral epithelial cells

1. Introduction

The COVID-19 pandemic remains a major public health crisis since the first case was reported in December 2019. Although severe acute respiratory syndrome-related coronavirus (SARS-CoV-2) vaccines are widely available, fully vaccinated people are not devoid of risk for infection by other variants of the virus [1-4]. Transmission of SARS-CoV-2 is known to occur through infected secretions, such as saliva and respiratory secretions, or their droplets [5]. Due to the mouth's proximity to the upper respiratory tract, salivary SARS-CoV-2 RNAs and proteins are detectable in infected symptomatic and

 doi:10.20944/preprints202303.0429.v1

asymptomatic individuals [6-9]. However, direct evidence supporting the oral cavity as a portal of SARS-CoV-2 entry is limited.

Previous studies indicate that human angiotensin-converting enzyme 2 (hACE2) acts as a primary SARS-CoV-2 receptor and can be used to predict cell susceptibility to infection by the virus [10]. Single-cell RNAseq analysis of oral tissues showed that hACE2 can be detected in various oral epithelial cell clusters although abundance is low except in salivary ducts [11]. Low numbers of hACE2 expressing cells are detected in buccal, tongue, and tonsil mucosa, suggesting that multiple sites in the oral cavity and oropharynx are potentially susceptible to infection by SARS-CoV-2 [11]. In this regard, Xu et al detected hACE2 expression in oral tissues, observing higher abundance in tongue than in buccal and gingival tissues [12]. Coincidentally, SARS-CoV-2 transcripts were detectable in salivary glands and in various mucosal sites (dorsal tongue, tonsil, and uvula) of COVID-19 autopsy tissues [11]. In addition to being detected in saliva, SARS-CoV-2 RNA was also detected in gingival crevicular fluid and oral plaque [13, 14], while SARS-CoV-2 spike proteins were observed histologically in cytological smears collected from the dorsum of the tongue of COVID-19 patients [15]. We have previously shown that TR146 cells, an oral epithelial cell line mimicking human buccal epithelium, are susceptible to pseudotyped viruses expressing SARS-CoV-2 spike proteins [16]; however, the susceptibility of TR146 cells and other oral epithelial cells including salivary gland and gingival epithelial cells to replication-competent viruses is not known. In this study, we determined the susceptibility of oral gingival epithelial cells, submaxillary salivary gland epithelial cells, and buccal oral epithelial cells to SARS-CoV-2.

2. Materials and Methods

2.1 Cell culture

HEK293T cells, Caco-2, Vero, oral gingival epithelium hTERT TIGKs (Telomerase Immortalized Gingival Keratinocytes, ATCC® CRL-3397), and submaxillary salivary gland A-253 (ATCC® HTB-41) were purchased from the American Type Cell Collection (ATCC, Manassas, VA). TR146 cells were purchased from Millipore Sigma. HEK293T, Caco-2, Vero, and hACE2-expressing HeLa cells (kindly provided by Dennis Burton; The Scripps Research Institute, La Jolla, CA) were cultured in Dulbecco's Modified Eagle's Medium (DMEM) supplemented with 10% fetal bovine serum (FBS). TR146 cells were cultured in Ham's F12 media with glutamate and 10% FBS. hTERT TIGKs cells were cultured in dermal cell basal medium (ATCC, PCS-200-030) with keratinocyte growth kits (ATCC, PCS-200-040). A-253 cells were cultured in McCoy's 5a medium with 10% FBS.

2.2 Viral infection assay

A replication-defective HIV-1 luciferase-expressing reporter virus pseudotyped with SARS-CoV2 S proteins were produced by co-transfection of a plasmid encoding the envelope-deficient HIV-1 NL4-3 virus with the luciferase reporter gene (pNL4-3.Luc.R+ E-, kindly provided by Nathaniel Landau, New York University) and a pcDNA3.1 plasmid expressing the SARS-CoV2 glycoprotein into HEK 293T cells using Lipofectamine 3000 (Thermo Fisher Scientific) as described previously [17]. The supernatant was collected 48 h after transfection and filtered. Virus stocks were analyzed for HIV-1 p24 antigen by the AlphaLISA HIV p24 kit (PerkinElmer). Virus stocks contained approximate 200 ng/ml of HIV p24 proteins. Cells were seeded at $5x10^4$ cells/well in a 48-well plate, cultured overnight, and infected with pseudotyped SARS-CoV-2 luciferase reporter virus. After 1-2 h viral attachment, infected cells were cultured in media with 10% FBS for 48-72 h. Cells were then lysed in 1x passive lysis buffer (Promega Inc.) followed by measuring luciferase activity (relative light units; RLUs) using Luciferase Substrate Buffer (Promega Inc.) on a 2300 EnSpire Multilabel Plate Reader (PerkinElmer).

The replication-competent SARS-CoV-2 USA-WA1/2020 strain (BEI Resources, ATCC) or Wuhan strain expressing mNeonGreen were propagated in Vero E6 cells as

Preprints (www.preprints.org) | NOT PEER-REVIEWED | Posted: 24 March 2023 doi:10.20944/preprints202303.0429.v1

described previously [18]. Experiments were performed in a Biosafety Level 3 laboratory with personal protection equipment including powered air purifying respirators (Breathe Easy, 3M), Tyvek suits, aprons, sleeves, booties, and double gloves. Virus titers were determined by plaque assays in Vero E6 cells as described previously [19]. For the plaque assay, Vero E6 cells were seeded in a 6-well plate at 6 x10^5 cells/well, cultured overnight, and then exposed to serial dilutions of viruses at 37°C for 1 h. After washing off unbound viruses, cells in each well were layered with a mixture of 1.5 ml of 1.6% of LE agarose (Sigma) and 1.5 ml of 2xDMEM with 4% FBS and 0.1% sodium bicarbonate and cultured for 3 days. Cells were then fixed with 10% formaldehyde and stained with crystal violet before counting plaque forming units.

2.3 Real-time RT-quantitative PCR analysis

Total RNA was isolated using TRIzol® (Life Technologies, Carlsbad, CA) followed by Zymo RNA isolation kits. SARS-CoV-2 RNA-dependent RNA polymerase gene (RdRP) and the SARS-CoV-2 nucleocapsid gene (N), together with the human β-actin gene as an internal control were quantified by RT-qPCR as described recently [20]. The reactions were carried out in a 20-μl volume that contained 1 x TaqPath 1-step RT-qPCR Master Mix (A28521, Thermo Fisher Scientific, Waltham, MA), 100 nM CoV-RdRP forward primer, 500 nM CoV-RdRP reverse primer, 250 nM CoV-RdRP molecular beacon probe, 100 nM CoV-N forward primer, 500 nM CoV-N reverse primer, 250 nM CoV-N molecular beacon probe, 100 nM β-actin forward primer, 500 nM β-actin reverse primer, and 250 nM β-actin molecular beacon probe. Total RNAs (1.5 μg) were used in each reaction. The RT-PCR assays were performed in 200 μl white polypropylene PCR tubes (USA Scientific, Ocala, FL) in a CFX96 Touch real-time PCR Detection System (Bio-Rad Laboratories, Hercules, CA). The thermal cycler was programed to incubate the reaction mixtures for 10 min at 53°C to generate cDNA, followed by 2 min at 95°C to activate the DNA polymerase and by 45 thermal cycles that consisted of DNA denaturation at 95°C for 15 sec and primer annealing and elongation at 58°C for 30 sec. Molecular beacon fluorescence intensity was monitored during the 58°C annealing and chain elongation stage of each thermal cycle. The primers and molecular beacons (Table 1) were purchased from LGC Biosearch Technologies (Middlesex, UK), and were modified and adapted from a previously validated assay [21].

Table 1. Primers and molecular beacon probes used in SARS-CoV-2 RT-PCR assay.

Oligonucleotide	Sequence 5' → 3'
CoV-RdRP forward	GTGARATGGTCATGTGTGGCGG
CoV-RdRP reverse	CARATGTTAAASACACTATTAGCATA
CoV-RdRP molecular beacon	FAM - CGCAG GGTGGAACCTCATCAGGAGATGC CTGCG - BHQ-1
CoV-N forward	GACCCCAAAATCAGCGAAAT
CoV-N reverse	TCTGGTTACTGCCAGTTGAATCTG
CoV-N molecular beacon	CFR - CGCGAG ACCCCGCATTACGTTTGGTGGACC CTCGCG - BHQ-2
β-actin forward	CCCAGCACAATGAAGATCAAGATC
β-actin reverse	AAGCATTTGCGGTGGACGAT
β-actin molecular beacon	Q705 - CGCCCG GCAAGCAGGAGTATGACGAGTCCGG CGGGCG - BHQ-2

FAM = fluorescein, CFR = Cal Fluor Red 610, Q705 = Quasar 705, BHQ = Black Hole Quencher, underlined nucleotides in molecular beacon probes indicate the 5' and 3' arm regions of the probe.

To determine the receptors for SARS-CoV-2, first-strand cDNA was synthesized by incubating 1000 ng total RNA with oligo(dT)$_{12-18}$ (25 μg/ml) and dNTP (0.5 mM) at 65°C for 5 min followed by quick-chilling on ice. RT was performed at 42°C for 50 min and 70°C for 15 min using SuperScript III Reverse Transcriptase. The PCR assay contained cDNA equivalent to 30 ng of RNA input, 200 nM primer sets, and SYBR Green Master Mix

 doi:10.20944/preprints202303.0429.v1

(QIAGEN, Valencia, CA), and was run in a StepOnePlus real-time PCR system (Life Technologies, Carlsbad, CA). PCR conditions included 95°C denaturation for 10 min, 40 cycles of 95°C for 15 sec and 60°C for 60 sec. PCR products were quantified and normalized relative to the amount of GAPDH cDNA products. Relative quantification of gene expression was calculated using the ΔΔCt (Ct, threshold cycle of real-time PCR) method according to the following formulas: ΔCT = Ct GAPDH − Ct target, ΔΔCt = ΔCt control − ΔCt target. Primer sequences were listed in Table 2.

Table 2. Primers used for RT-qPCR assays for host genes.

Primer	Forward	Reverse
Human GAPDH	5′- GCACCACCAACTGCTTAGCAC-3′	5′-TCTTCTGGGTGGCAGTGATG-3′
Human ACE2	5′-CGAAGCCGAAGACCTGTTCTA-3′	5′-GGGCAAGTGTGGACTGTTCC-3′
Human TMPRSS2	5′-CAAGTGCTCCAACTCTGGGAT-3′	5′- AACACACCGATTCTCGTCCTC-3′
Human TMPRSS4	5′- CCAAGGACCGATCCACAC T-3′	5′- GTGAAGTTGTCGAAACAGGCA-3′;
Human CD147	5′-GTC TTC CTC CCC GAG CCC-3′	5′-GGTGGCACGGACTCTGAC-3′
Human AXL	5′-GTGGGCAACCCAGGGAATATC-3′	5′-GTACTG TCCCGTGTCG GAAAG-3′

2.4 Single molecule Fluorescence In Situ Hybridization (smFISH)

smFISH for SARS-CoV-2 RNA was performed following procedures described previously [22]. We designed a total of 336 3′-amino labeled oligonucleotide probes for the SARS-CoV-2 genomic RNA using Stellaris Probe Designer employing highest stringency settings for human host, pooled all probes, coupled them to Cy5, and then purified them using HPLC [23]. Cells were cultured on coverslips coated with 0.1% gelatin in 12-well plates for overnight and then exposed to SARS-CoV-2 viruses expressing GFP at a multiplicity of infection (MOI) of 0.5 for 1 h. At 24 and 48 h post-infection, cells on the coverslips were washed with PBS, and then fixed with 10% formaldehyde in 1X PBS for 10 min, washed with PBS, and stored in 70% ethanol at -20°C. The coverslips were equilibrated with 2XSSC, 10% formamide (wash buffer) before hybridization and then hybridized in 50 μl hybridization buffer supplemented with 25 ng of pooled probes overnight at 37°C in a humid chamber. The coverslips were washed twice for 5 min with the wash buffer, equilibrated with 2XSSC supplemented with 0.4% glucose, and then mounted using deoxygenated mounting medium supplemented with DAPI [22]. Approximate 20 images per sample were acquired using a Zeiss Axiovert M200 microscope with a 20X objective.

2.5 Statistical analysis

Statistical comparisons were performed using one-way ANOVA Dunnett's multiple comparisons test or two-tailed Mann-Whitney U test as appropriate. Prism 8 (GraphPad Software, LLC) was used. $p < 0.05$ was considered significant.

3. Results

3.1 Expression of hACE2 and alternative receptors CD147 and AXL

hACE2 has been considered to be a determinant of SARS-CoV-2 cell and tissue tropism via the receptor-binding domain (RBD) in the surface/spike protein. Additionally, transmembrane protease serine 2 (TMPRSS2) and 4 (TMPRSS4) interact with SARS-CoV-2 spike proteins and promote hACE2-mediated viral entry [10, 24]. We determined expression of hACE2, TMPRSS2, and TMPRSS4 mRNA in oral gingival epithelial cells (hTERT TIGKs), submaxillary salivary gland A-253 cells, and oral buccal epithelial TR146 cells. HEK293T cells, which were used in our previous analyses for hACE2 expression in

Preprints (www.preprints.org) | NOT PEER-REVIEWED | Posted: 24 March 2023 doi:10.20944/preprints202303.0429.v1

various cell lines and which were not permissive for SARS-CoV-2 [17], were included for comparison. All oral epithelial cells analyzed in this study expressed low levels of hACE2 mRNAs (Fig 1A). In hTERT TIGKs, hACE2 expression was nearly undetectable. Gene expression profiles of TMPRSS2 and TMPRSS4 varied among oral epithelial cells. A-253 cells expressed both TMPRSS2 and TMPRSS4, whereas hTERT TIGKs had detectable TMPRSS2 but low levels of TMPRSS4. TR146 cells had low abundance of TMPRSS2 but high abundance of TMPRSS4.

Alternative receptors for SARS-CoV-2 viral entry including CD147 (known as *basigin* or EMMPRIN) and AXL (tyrosine-protein kinase receptor UFO) have also been reported, particularly in cells with low abundance hACE2 [25-27]. We have previously shown that SARS-CoV-2 infects cells with low abundance of hACE2 via CD147 in a spike RBD-independent manner [17]. RT-qPCR analyses of CD147 and AXL mRNAs showed that all oral epithelial cells expressed high levels of CD147 (Fig 1B). AXL mRNAs were expressed in hTERT TIGKs and TR146 cells but were nearly undetectable in A-253 cells.

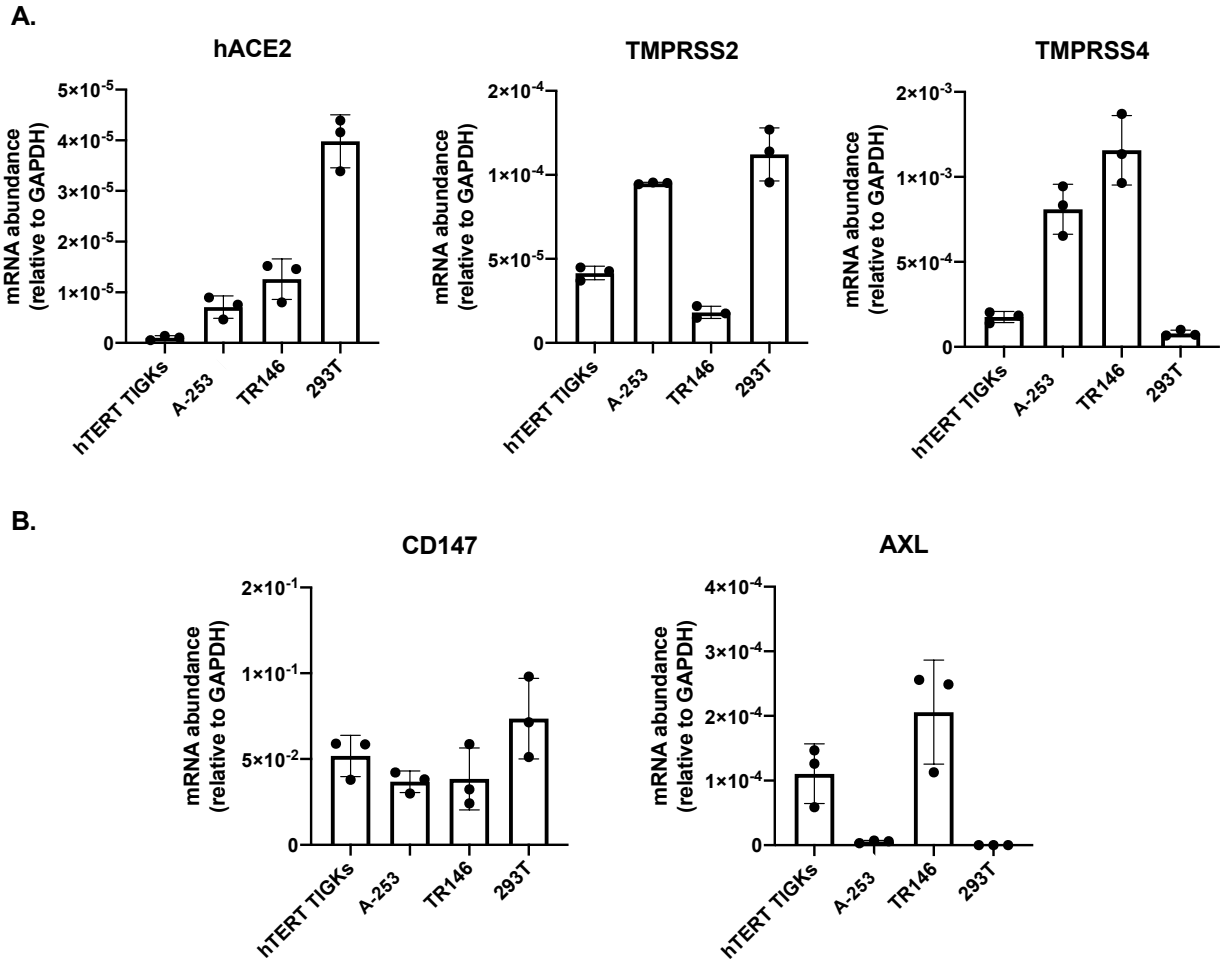

Figure 1. Expression of hACE2, TMPRSS2, TMPRSS4, CD147, and AXL mRNA in oral epithelial cell lines. Total RNAs were extracted from oral gingival epithelial cells (hTERT TIGKs), salivary gland epithelial cells (A-253), oral buccal epithelial cells (TR146) and HEK293T cells. (A) Expression of hACE2, TMPRSS2, TMPRSS4. (B) Expression of hACE2-independent alternative receptors CD147 (*left*) and AXL (*right*). GAPDH was used for normalization.

3.2 Various oral epithelial cell lines are susceptible to SARS-CoV-2

To determine whether oral epithelial cells representing different sites of the oral cavity were susceptible to SARS-CoV-2, and pseudotyped luciferase reporter viruses

Preprints (www.preprints.org) | NOT PEER-REVIEWED | Posted: 24 March 2023 doi:10.20944/preprints202303.0429.v1

expressing SARS-CoV-2 spike proteins were tested in the viral entry assay. hTER TIGKs, A-253, and TR146 cells were susceptible to the SARS-CoV-2 pseudotyped virus (Fig 2A), but the degree of infection did not correlate with hACE2 expression (Fig 1A).

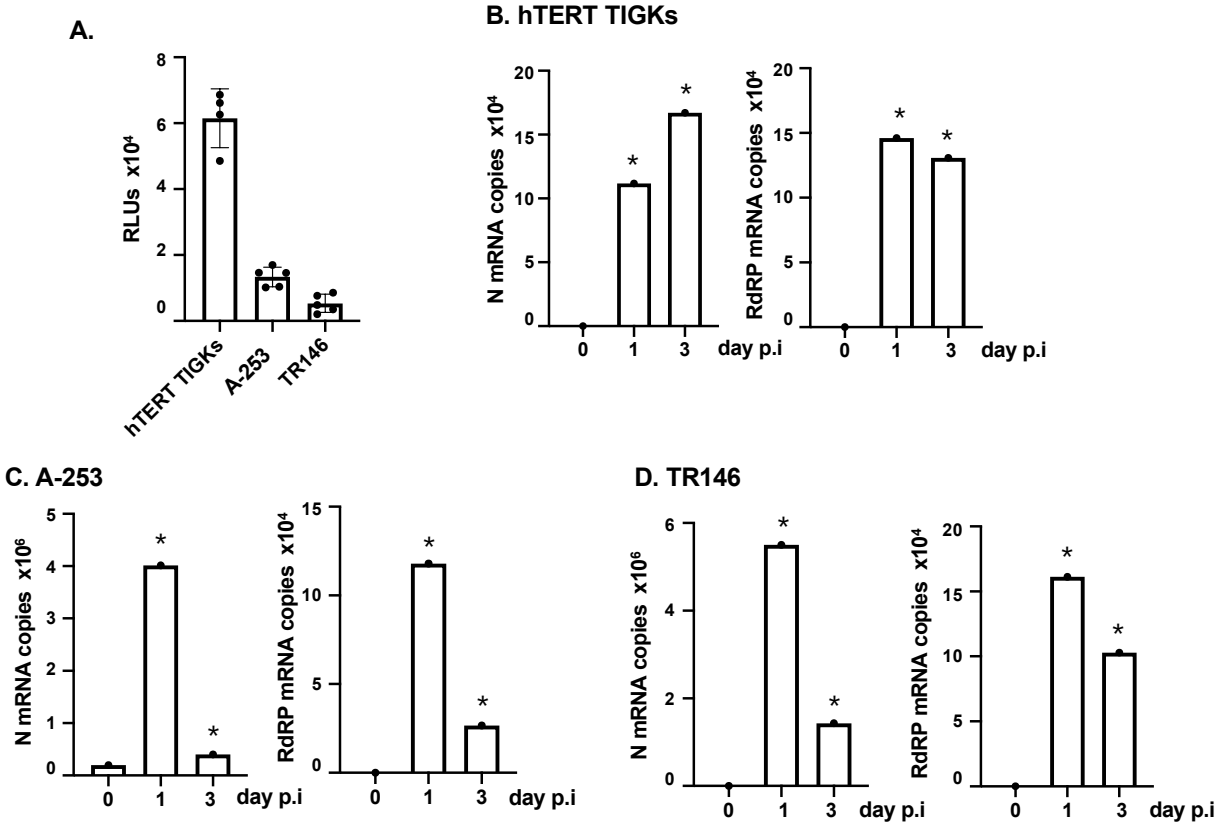

Figure 2. Infection of oral epithelial cells by pseudotyped SARS-CoV-2 virus or by replication competent SARS-CoV-2 WA 01/2020 strain. (A) Oral gingival epithelial cells (hTERT TIGKs), salivary gland epithelial cells (A-253), and oral buccal epithelial cells (TR146) were infected by pseudotyped SARS-CoV-2 viruses. Infection was determined by measuring luciferase activity at 72 h after infection. (B-D) Oral epithelial cells were exposed to replication competent SARS-CoV-2 WA 01/2020 strain at an MOI of 0.5 for 1 h, washed with PBS, and placed in culture. Total RNAs were prepared at 2 h (day 0), day 1, and day 3 p.i. SARS-CoV-2 N and RdRP mRNA copy numbers and b-actin were analyzed by RT-qPCR. Copy numbers from approximately $1x10^5$ cells are shown. Data are mean ± SD; *p<0.05, infected samples vs the day 0 sample.

We then infected oral epithelial cells with replication competent SARS-CoV-2 WA strains at a MOI 0.5. Total RNAs from infected cells were prepared at 2 h, 1 d, and 3 d post-infection (p.i). SARS-CoV-2 N (nucleocapsid) and RdPR (RNA-dependent RNA polymerase) transcripts were determined by RT-qPCR analysis. There was an increase in both SARS-CoV-2 transcripts on day 1 compared to 2 h (day 0) p.i., indicating productive viral replication. At day 3 p.i., the levels of viral transcripts were sustained in hTERT TIGKs but were significantly decreased in A-253 and TR146 cells (Fig 2B-D). Note that viral transcripts among total RNA of the population of infected cells were measured; thus, reduction of viral mRNA was unlikely due to virus-induced cell death.

Oral epithelial cells were then infected with replication competent SARS-CoV-2 viruses expressing GFP. In addition to visualizing GFP signals, SARS-CoV-2 RNAs were also analyzed by smFISH. Overall, the signals of GFP and SARS-CoV-2 mRNAs were co-localized in the same cells (Fig 3). Both GFP proteins and SARS-CoV-2 RNAs were detectable at 24 h p.i. and the signals were not increased at 48 h p.i. (data not shown for 24 h

 doi:10.20944/preprints202303.0429.v1

p.i.). Regardless of the type of oral epithelial cells, the viral signal was low in most cells. However, a few cells, typically one cell per field of view, had high viral signals. We found single cells with viral mRNAs rather than two adjacent infected cells, suggesting the absence of cell-cell viral transmission. Occasionally we observed two infected cells that were adjacent to each other, which could arise due to cell division after infection. We conclude that hTER TIGKs, A-253, and TR146 cells were susceptible to SARS-CoV-2 (Figs 2-3) but the viral dynamics in hTER TIGKs differed from those in A-253 and TR146 cells, as mRNA levels were maintained in hTER TIGKs (Fig 2B) but decreased rapidly from day 1 to day 3 in A-253 (Fig 2C) and TR146 cells (Fig 2D).

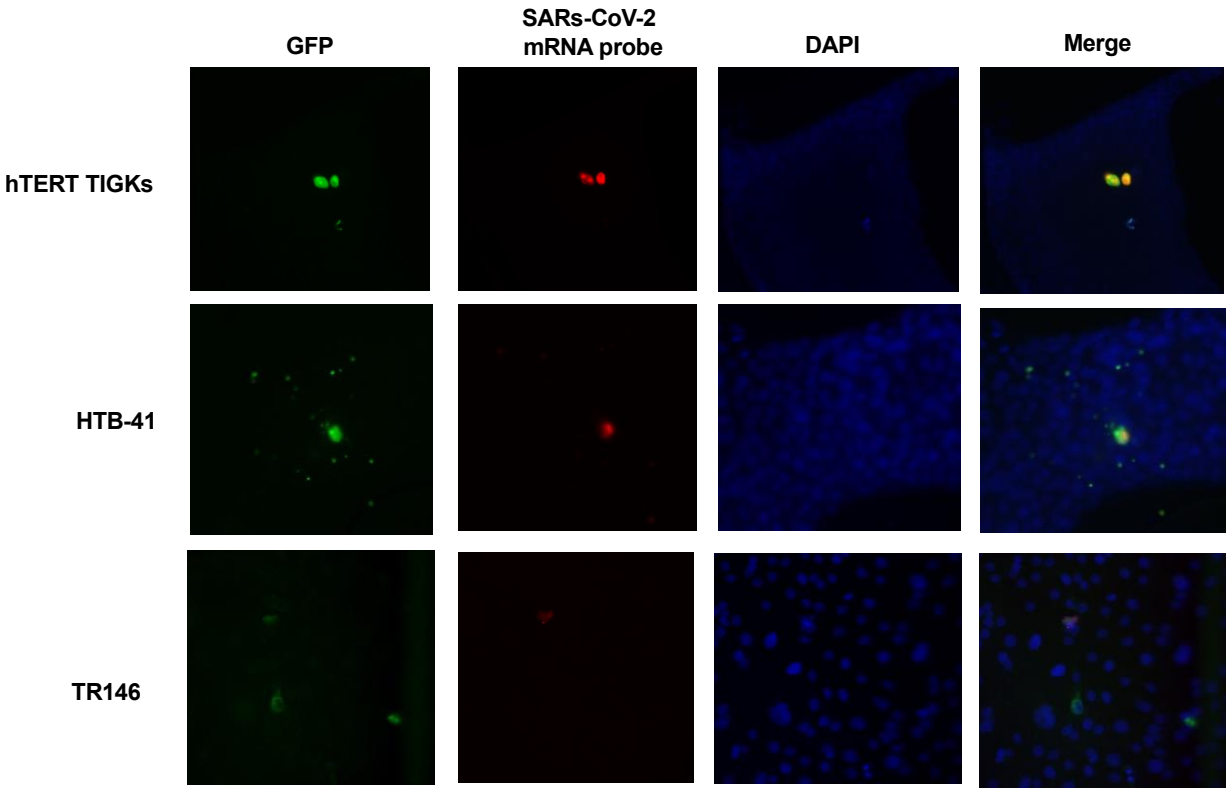

Figure 3. Infection of oral epithelial cells by replication competent SARS-CoV-2 Wuhan strain expressing GFP. Oral gingival epithelial cells (hTERT TIGKs), salivary gland epithelial cells (A-253), and oral buccal epithelial cells (TR146) were infected by SARS-CoV-2 Wuhan strain expressing GFP. Infection was determined by detecting fluorescence (GFP) and by smFISH with SARS-CoV-2 mRNA probes at 48 h p.i. Nuclei were stained with DAPI. Images were acquired on a Zeiss Axiovert M200 microscope with a 20X objective.

4. Discussion

The oral cavity is considered a gateway for many pathogens, like SARS-CoV-2, that can infect the human body; however, there is limited evidence supporting SARS-CoV-2 replication in oral epithelial cells. Here, we found that oral gingival epithelial cells (hTERT TIGKs), salivary gland epithelial cells (A-253), and oral buccal epithelial cells (TR146) were susceptible to infection by both a pseudotyped virus expressing SARS-CoV-2 spike proteins and by replication competent SARS-CoV-2.

Assays for SARS-CoV-2 infection of oral epithelial cells have mainly relied on the detection of viral transcripts or proteins in oral tissues from COVID-19 patients. Here, in experiments using a variety of SARS-CoV-2 virus forms including pseudotyped viruses expressing SARS-CoV-2 spike proteins (for viral entry), replication competent SARS-CoV-2 viruses, and SARS-CoV-2 viruses expressing GFP, we showed that SARS-CoV-2 infected oral gingival epithelial cells (hTERT TIGKs), salivary gland epithelial cells (A-253), and

 doi:10.20944/preprints202303.0429.v1

oral buccal epithelial cells (TR146). Viral transcripts were detected by RT-qPCR and smFISH. In agreement with previous results in oral tissues from COVID-patients [11], a few cells expressed high levels of SARS-CoV-2 mRNAs and GFP proteins. The viral signal remained high at day 3 p.i. in hTERT TIGKs but decreased significantly at day 3 p.i. in A-253 and TR146. SARS-CoV-2 N mRNA copy numbers in A-253 and TR146 were higher than in hTERT TIGKs (4-5.5x10^6 vs 1x10^6 copies/10^5 cells). hTERT TIGKs, which are telomerase immortalized cells, were also less transformed than A-253 and TR146, which are tumor-derived cell lines. It remains to be determined whether the cells derived from different sites within the oral cavity or the degree of tumorgenicity contribute to differential infection profiles. It is worth noting that all oral epithelial cells expressed low levels of hACE2, and the hACE mRNA level did not correlate with the extent of pseudotyped SARS-CoV-2 virus entry. All oral epithelial cells expressed highly abundant CD147, an alternative receptor, and hTERT TIGKs and A-235 cells also expressed AXL, another alternative receptor. SARS-CoV-2 viral entry via CD147 and AXL is known to be independent of hACE2 spike RBD proteins [17, 26], which are the targets of current vaccines. In addition to CD147 and AXL, other hACE2-independent receptors for SARS-CoV-2 have been reported (reviewed in [28]). Further studies on expression profiles of alternative receptors and specific receptors and factors promoting SARS-CoV-2 viral entry into oral epithelial cells, as well as studies on virus-mediated alterations of oral epithelial cell functions, will provide a better understanding of SARS-CoV-2 pathogenesis in the oral cavity.

Acknowledgments: This work was funded by the Colgate Palmolive Co. TLC and DHF were also supported by NIH grant numbers R01AI36948 and NIH R01DE017968, respectively. ST and SAEM were supported by NIH grant R01CA227291.

References

1. Pak, A.; Adegboye, O. A.; Adekunle, A. I.; Rahman, K. M.; McBryde, E. S.; Eisen, D. P., Economic Consequences of the COVID-19 Outbreak: the Need for Epidemic Preparedness. *Frontiers in Public Health* **2020,** 8.
2. Rahman, S.; Rahman, M. M.; Miah, M.; Begum, M. N.; Sarmin, M.; Mahfuz, M.; Hossain, M. E.; Rahman, M. Z.; Chisti, M. J.; Ahmed, T.; Arifeen, S. E.; Rahman, M., COVID-19 reinfections among naturally infected and vaccinated individuals. *Scientific Reports* **2022,** 12, (1), 1438.
3. Jeffery-Smith, A.; Rowland, T. A. J.; Patel, M.; Whitaker, H.; Iyanger, N.; Williams, S. V.; Giddings, R.; Thompson, L.; Zavala, M.; Aiano, F.; Ellis, J.; Lackenby, A.; Höschler, K.; Brown, K.; Ramsay, M. E.; Gopal, R.; Chow, J. Y.; Ladhani, S. N.; Zambon, M., Reinfection with new variants of SARS-CoV-2 after natural infection: a prospective observational cohort in 13 care homes in England. *The Lancet Healthy Longevity* **2021,** 2, (12), e811-e819.
4. Nguyen, N. N.; Houhamdi, L.; Hoang, V. T.; Delerce, J.; Delorme, L.; Colson, P.; Brouqui, P.; Fournier, P. E.; Raoult, D.; Gautret, P., SARS-CoV-2 reinfection and COVID-19 severity. *Emerg Microbes Infect* **2022,** 11, (1), 894-901.
5. WHO, Transmission of SARS-CoV-2: implication for infection prevention precautions. World Health Organization https://www.who.int/news-room/commentaries/detail/transmission-of-sars-cov-2-implications-for-infection-prevention-precautions **2020**.
6. To, K. K.; Tsang, O. T.; Leung, W. S.; Tam, A. R.; Wu, T. C.; Lung, D. C.; Yip, C. C.; Cai, J. P.; Chan, J. M.; Chik, T. S.; Lau, D. P.; Choi, C. Y.; Chen, L. L.; Chan, W. M.; Chan, K. H.; Ip, J. D.; Ng, A. C.; Poon, R. W.; Luo, C. T.; Cheng, V. C.; Chan, J. F.; Hung, I. F.; Chen, Z.; Chen, H.; Yuen, K. Y., Temporal profiles of viral load in posterior oropharyngeal saliva samples and serum antibody responses during infection by SARS-CoV-2: an observational cohort study. *Lancet Infect Dis* **2020,** 20, (5), 565-574.
7. Wei, L.; Lin, J.; Duan, X.; Huang, W.; Lu, X.; Zhou, J.; Zong, Z., Asymptomatic COVID-19 Patients Can Contaminate Their Surroundings: an Environment Sampling Study. *mSphere* **2020,** 5, (3).
8. Lee, S.; Kim, T.; Lee, E.; Lee, C.; Kim, H.; Rhee, H.; Park, S. Y.; Son, H.-J.; Yu, S.; Park, J. W.; Choo, E. J.; Park, S.; Loeb, M.; Kim, T. H., Clinical Course and Molecular Viral Shedding Among Asymptomatic and Symptomatic Patients With SARS-CoV-2 Infection in a Community Treatment Center in the Republic of Korea. *JAMA Internal Medicine* **2020**.
9. Pijuan-Galito, S.; Tarantini, F. S.; Tomlin, H.; Jenkins, H.; Thompson, J. L.; Scales, D.; Stroud, A.; Tellechea Lopez, A.; Hassall, J.; McTernan, P. G.; Coultas, A.; Arendt-Tranholm, A.; Reffin, C.; Hill, I.; Lee, I.-n.; Wu, S.; Porte, J.; Chappell, J.; Lis-Slimak, K.; Kaneko, K.; Doolan, L.; Ward, M.; Stonebridge, M.; Ilyas, M.; McClure, P.; Tighe, P.; Gwynne, P.; Hyde, R.; Ball, J.; Seedhouse, C.; Benest, A. V.; Petrie, M.; Denning, C., Saliva for COVID-19 Testing: Simple but Useless or an Undervalued Resource? *Frontiers in Virology* **2021,** 1.

10. Hoffmann, M.; Kleine-Weber, H.; Schroeder, S.; Kruger, N.; Herrler, T.; Erichsen, S.; Schiergens, T. S.; Herrler, G.; Wu, N. H.; Nitsche, A.; Muller, M. A.; Drosten, C.; Pohlmann, S., SARS-CoV-2 Cell Entry Depends on ACE2 and TMPRSS2 and Is Blocked by a Clinically Proven Protease Inhibitor. *Cell* **2020,** 181, (2), 271-280 e8.
11. Huang, N.; Pérez, P.; Kato, T.; Mikami, Y.; Okuda, K.; Gilmore, R. C.; Conde, C. D.; Gasmi, B.; Stein, S.; Beach, M.; Pelayo, E.; Maldonado, J. O.; Lafont, B. A.; Jang, S.-I.; Nasir, N.; Padilla, R. J.; Murrah, V. A.; Maile, R.; Lovell, W.; Wallet, S. M.; Bowman, N. M.; Meinig, S. L.; Wolfgang, M. C.; Choudhury, S. N.; Novotny, M.; Aevermann, B. D.; Scheuermann, R. H.; Cannon, G.; Anderson, C. W.; Lee, R. E.; Marchesan, J. T.; Bush, M.; Freire, M.; Kimple, A. J.; Herr, D. L.; Rabin, J.; Grazioli, A.; Das, S.; French, B. N.; Pranzatelli, T.; Chiorini, J. A.; Kleiner, D. E.; Pittaluga, S.; Hewitt, S. M.; Burbelo, P. D.; Chertow, D.; Kleiner, D. E.; De Melo, M. S.; Dikoglu, E.; Desar, S.; Ylaya, K.; Chung, J.-Y.; Smith, G.; Chertow, D. S.; Vannella, K. M.; Ramos-Benitez, M.; Ramelli, S. C.; Samet, S. J.; Babyak, A. L.; Valenica, L. P.; Richert, M. E.; Hays, N.; Purcell, M.; Singireddy, S.; Wu, J.; Chung, J.; Borth, A.; Bowers, K.; Weichold, A.; Tran, D.; Madathil, R. J.; Krause, E. M.; Herr, D. L.; Rabin, J.; Herrold, J. A.; Tabatabai, A.; Hochberg, E.; Cornachione, C.; Levine, A. R.; McCurdy, M. T.; Saharia, K. K.; Chancer, Z.; Mazzeffi, M. A.; Richards, J. E.; Eagan, J. W.; Sangwan, Y.; Sequeira, I.; A. Teichmann, S.; J. Kimple, A.; Frank, K.; Lee, J.; Boucher, R. C.; Teichmann, S. A.; Warner, B. M.; Byrd, K. M.; Consortium, N. C.-A.; Oral, H. C. A.; Craniofacial Biological, N., SARS-CoV-2 infection of the oral cavity and saliva. *Nature medicine* **2021,** 27, (5), 892-903.
12. Xu, H.; Zhong, L.; Deng, J.; Peng, J.; Dan, H.; Zeng, X.; Li, T.; Chen, Q., High expression of ACE2 receptor of 2019-nCoV on the epithelial cells of oral mucosa. *International Journal of Oral Science* **2020,** 12, (1), 8.
13. Gupta, S.; Mohindra, R.; Chauhan, P. K.; Singla, V.; Goyal, K.; Sahni, V.; Gaur, R.; Verma, D. K.; Ghosh, A.; Soni, R. K.; Suri, V.; Bhalla, A.; Singh, M. P., SARS-CoV-2 Detection in Gingival Crevicular Fluid. *J Dent Res* **2021,** 100, (2), 187-193.
14. Gomes, S. C.; Fachin, S.; da Fonseca, J. G.; Angst, P. D. M.; Lamers, M. L.; da Silva, I. S. B.; Nunes, L. N., Dental biofilm of symptomatic COVID-19 patients harbours SARS-CoV-2. *J Clin Periodontol* **2021,** 48, (7), 880-885.
15. Marques, B. B. F.; Guimarães, T. C.; Fischer, R. G.; Tinoco, J. M. M.; Pires, F. R.; Lima Junior, J. d. C.; Stevens, R. H.; Tinoco, E. M. B., Morphological alterations in tongue epithelial cells infected by SARS-CoV-2: A case–control study. *Oral Diseases* n/a, (n/a).
16. Xu, C.; Wang, A.; Hoskin, E. R.; Cugini, C.; Markowitz, K.; Chang, T. L.; Fine, D. H., Differential Effects of Antiseptic Mouth Rinses on SARS-CoV-2 Infectivity In Vitro. *Pathogens* **2021,** 10, (3).
17. Xu, C.; Wang, A.; Geng, K.; Honnen, W.; Wang, X.; Bruiners, N.; Singh, S.; Ferrara, F.; D'Angelo, S.; Bradbury, A. R. M.; Gennaro, M. L.; Liu, D.; Pinter, A.; Chang, T. L., Human Immunodeficiency Viruses Pseudotyped with SARS-CoV-2 Spike Proteins Infect a Broad Spectrum of Human Cell Lines through Multiple Entry Mechanisms. *Viruses* **2021,** 13, (6).
18. Xie, X.; Muruato, A.; Lokugamage, K. G.; Narayanan, K.; Zhang, X.; Zou, J.; Liu, J.; Schindewolf, C.; Bopp, N. E.; Aguilar, P. V.; Plante, K. S.; Weaver, S. C.; Makino, S.; LeDuc, J. W.; Menachery, V. D.; Shi, P. Y., An Infectious cDNA Clone of SARS-CoV-2. *Cell Host Microbe* **2020,** 27, (5), 841-848 e3.
19. Xu, C.; Wang, A.; Hoskin, E. R.; Cugini, C.; Markowitz, K.; Chang, T. L.; Fine, D. H., Differential Effects of Antiseptic Mouth Rinses on SARS-CoV-2 Infectivity In Vitro. *Pathogens* **2021,** 10, (3), 272.
20. Dikdan, R. J.; Marras, S. A. E.; Field, A. P.; Brownlee, A.; Cironi, A.; Hill, D. A.; Tyagi, S., Multiplex PCR Assays for Identifying all Major Severe Acute Respiratory Syndrome Coronavirus 2 Variants. *J Mol Diagn* **2022,** 24, (4), 309-319.
21. Corman, V. M.; Landt, O.; Kaiser, M.; Molenkamp, R.; Meijer, A.; Chu, D. K.; Bleicker, T.; Brunink, S.; Schneider, J.; Schmidt, M. L.; Mulders, D. G.; Haagmans, B. L.; van der Veer, B.; van den Brink, S.; Wijsman, L.; Goderski, G.; Romette, J. L.; Ellis, J.; Zambon, M.; Peiris, M.; Goossens, H.; Reusken, C.; Koopmans, M. P.; Drosten, C., Detection of 2019 novel coronavirus (2019-nCoV) by real-time RT-PCR. *Euro Surveill* **2020,** 25, (3).
22. Raj, A.; van den Bogaard, P.; Rifkin, S. A.; van Oudenaarden, A.; Tyagi, S., Imaging individual mRNA molecules using multiple singly labeled probes. *Nat Methods* **2008,** 5, (10), 877-9.
23. Raj, A.; Tyagi, S., Detection of individual endogenous RNA transcripts in situ using multiple singly labeled probes. *Methods Enzymol* **2010,** 472, 365-86.
24. Zang, R.; Gomez Castro, M. F.; McCune, B. T.; Zeng, Q.; Rothlauf, P. W.; Sonnek, N. M.; Liu, Z.; Brulois, K. F.; Wang, X.; Greenberg, H. B.; Diamond, M. S.; Ciorba, M. A.; Whelan, S. P. J.; Ding, S., TMPRSS2 and TMPRSS4 promote SARS-CoV-2 infection of human small intestinal enterocytes. *Sci Immunol* **2020,** 5, (47).
25. Wang, K.; Chen, W.; Zhang, Z.; Deng, Y.; Lian, J.-Q.; Du, P.; Wei, D.; Zhang, Y.; Sun, X.-X.; Gong, L.; Yang, X.; He, L.; Zhang, L.; Yang, Z.; Geng, J.-J.; Chen, R.; Zhang, H.; Wang, B.; Zhu, Y.-M.; Nan, G.; Jiang, J.-L.; Li, L.; Wu, J.; Lin, P.; Huang, W.; Xie, L.; Zheng, Z.-H.; Zhang, K.; Miao, J.-L.; Cui, H.-Y.; Huang, M.; Zhang, J.; Fu, L.; Yang, X.-M.; Zhao, Z.; Sun, S.; Gu, H.; Wang, Z.; Wang, C.-F.; Lu, Y.; Liu, Y.-Y.; Wang, Q.-Y.; Bian, H.; Zhu, P.; Chen, Z.-N., CD147-spike protein is a novel route for SARS-CoV-2 infection to host cells. *Signal Transduction and Targeted Therapy* **2020,** 5, (1), 283.
26. Wang, S.; Qiu, Z.; Hou, Y.; Deng, X.; Xu, W.; Zheng, T.; Wu, P.; Xie, S.; Bian, W.; Zhang, C.; Sun, Z.; Liu, K.; Shan, C.; Lin, A.; Jiang, S.; Xie, Y.; Zhou, Q.; Lu, L.; Huang, J.; Li, X., AXL is a candidate receptor for SARS-CoV-2 that promotes infection of pulmonary and bronchial epithelial cells. *Cell Research* **2021,** 31, (2), 126-140.
27. Xu, C.; Wang, A.; Geng, K.; Honnen, W.; Wang, X.; Bruiners, N.; Singh, S.; Ferrara, F.; D'Angelo, S.; Bradbury, A. R. M.; Gennaro, M. L.; Liu, D.; Pinter, A.; Chang, T. L., Human Immunodeficiency-1 Pseudotyped Viruses Expressing SARS-CoV-2 Spike Proteins Infect a Broad Spectrum of Human Cell Lines Through Multiple Entry Mechanisms. *Viruses* **2021,** 13.
28. Lim, S.; Zhang, M.; Chang, T. L., ACE2-independent alternative receptors for SARS-CoV-2. *Viruses* **2022,** 14, (11), 2535.